Border Reactivity of Polycyclic Aromatic Hydrocarbons and Soot Platelets Toward Ozone. A Theoretical Study

UNIVERSITÀ DEGLI STUDI DI TORINO

Border Reactivity of Polycyclic Aromatic Hydrocarbons and Soot Platelets Towards Ozone. A Theoretical Study

Anna Giordana,[1] Andrea Maranzana,[1] Giovanni Ghigo,[1] Mauro Causà,[2,*] and Glauco Tonachini[1,*]

Dipartimento di Chimica Generale e Chimica Organica, Università di Torino, Corso Massimo D'Azeglio 48, I-10125 Torino, Italy,
and
Dipartimento di Chimica, Università di Napoli "Federico II", Complesso Universitario di Monte Sant'Angelo, Via Cintia 1, I-80126 Napoli, Italy

Abstract. PAH-based models, with an even or odd number of unsaturated carbon atoms and π electrons (*even* and *odd* PAHs for short), have been selected to investigate, by molecular and periodic methods, their electron distribution and border reactivity towards ozone, and also to represent local features and edge reactivity of *even* or *odd* soot platelets. Their topologically different perimeter positions, representative of armchair and zigzag borders, exhibit different reactivity right from the beginning. Ozone attacks start off either to give primary ozonides by concerted addition, or, non-concertedly, to first produce trioxyl intermediates. Then, a variety of pathways are described, whose viability depends both on model and position. They can open the way to the possible formation of epoxidic, aldehydic, and phenolic groups (all entailing O_2 production), or ether (+ CO_2), lactone (+ H_2CO), and ketonic functionalities. To sum up, functionalization, regardless of how achieved, can give a number of groups, most of which actually observed in PAH ozonization experimental studies. This picture can be compared with our previous results on internal sites, for which epoxidation was the only outcome. Most interestingly, formation of a ketonic group may turn an even system into an odd one (and conversely) while involving production of $HOO^{\bullet}$.

[1] Università di Torino [2] Università di Napoli

keywords: polycyclic aromatic hydrocarbons / PAH / soot / border / ozonization

* corresponding authors:

e-mail addresses	fax	web sites:
glauco.tonachini@unito.it	++39-011-236 7648	http://www.thecream.unito.it/
mauro.causa@unina.it	++39-081-674 090	http://www.mfn.unipmn.it/~causa

1. Introduction

Soot aerosol contributes significantly to the mass of atmospheric aerosol, since great quantities of elemental carbon are generated by biomass and fossil fuel combustion and emitted into the troposphere.[1] Soot is made up by clustered globular particles, composed in turn by irregular and curved graphenic layers, or platelets, which can be stacked to form small *crystallites* (turbostratic structure).[2] The particles' features, as regards structure and composition, depend on their origin[3a,4] and history,[5] and its surface is available to interactions with a variety of airborne inorganic and organic molecules.

Polycyclic aromatic hydrocarbons (PAHs) and their derivatives (PACs, polycyclic aromatic compounds) are also generated by combustion. PAH oxidation can also take place at a later time, during the tropospheric transport.[3] PAHs and PACs share origin and structural affinities with soot,[3,4a] and their oxidation could share some mechanistic features. Also the oxidation of PAHs on soot has been investigated experimentally.[6] In fact, PAHs and PACs are frequently found in association to carbonaceous particulate,[3b,7,8] and PACs have been supposed to possibly originate on the surface of particulate matter, since they have been detected in diesel exhaust. Several laboratory studies on the interaction of soot with small inorganic oxidants, as NO_2,[6,9,10,11] HNO_3,[9] H_2O,[7,11,12] and O_3,[13,14,15,16] have been carried out. Also studies focused on the reaction of ozone with PAHs in the gas phase, in solution, or adsorbed under different conditions can be mentioned.[7,17,18]

Functionalization can in particular bring about a polarity increase of the primary pollutants (compounds or particles), and consequently of its water solubility. As a result, the aerosol carries them more easily into contact with, for example, the lung tissues. Therefore, PAHs and PACs adsorbed on fine particles are of concern as regards human health. PAHs have been shown to decay at different rates, while transported:[19] as other products form, the relative amount of carcinogenic or mutagenic compounds can change extensively, and the nature of these secondary pollutants is not known in all cases.[20] Gas phase reactions and heterogeneous processes by which primary pollutants can transform is thus unmistakably of chemical and toxicologic interest.

The theoretical study of the interaction of O_3 with PAHs or with the surface of ideal soot particles can be helpful to better understand the results of laboratory studies. The reaction paths studied by theoretical methods are in fact pertinent to gas-phase reactions, such as those already examined in this laboratory.[21] It must be mentioned that the theoretical modeling of soot has also been the goal of other groups in recent years.[22,23,24,25,26,27]

To better introduce the present study, we can briefly recall some previous work of our group on this subject. In the first study,[28] we attempted to define a suitable model for soot, and examined its interaction with some small species. Then we have focused on the ozonization mechanism for some PAHs containing an even number of carbon atoms (*even* PAHs), and only for internal positions, considering these attacks as carried out on exposed internal zones of soot platelets.[29] We have also explored the nature of the oxidized soot surface through the theoretical study of the desorption mechanisms of an assortment of functional groups, and attempted to give a contribution to the interpretation of Temperature Programmed Desorption (TPD) spectra.[30] Since PAHs made by an odd or even number of unsaturated carbon atoms and π electrons (*odd* or *even* PAHs)[31] have been found to have approximately the same quantitative importance in flames, in particular beyond 25 carbon atoms,[4a,c] and soot platelets constituted by an odd number of carbon atoms can be reasonably assumed to form during combustion, we have also addressed the same problem for these systems.[32]

In the present paper, quantum mechanical calculations are initially carried out on molecular *even* and *odd* PAH systems, then expanded to some extent to periodic systems, in order to complete the picture provided by the preceding studies just mentioned. Therefore, the reactivity of selected PAH border positions with ozone, recognized as an important atmospheric oxidant for organics, and the relevant mechanistic traits, are investigated and compared with the features exhibited by internal positions. PAHs are studied here as systems interesting *per se*, but also intended as suitable small models to investigate the local features and the border reactivity of exposed soot platelets. To this purpose, the ozonization mechanism is investigated by the same approach already adopted for the internal positions of even and odd systems.[29,32]

2. Methods

The stable and transition structures (TS) are determined by gradient procedures,[33] within the Density Functional Theory (DFT).[34] The B3LYP functional was chosen, which is of widespread use, and, although prone to underestimate some reaction barriers, has generally performed satisfactorily as regards geometries and energetics.[35] Given the large number of structures studied, and for sake of uniformity with the preceding papers,[29-30] no other functionals were used. The polarized 6-31G(d)[36a] basis set was used in the DFT (B3LYP) optimizations. The nature of the critical points was checked by vibrational analysis. For transition structures (TS), corresponding to first-order saddle points, inspection of the normal

mode related to the imaginary frequency was in most cases sufficient to confidently establish its connection with the initial and final stable species, which correspond to energy minima. The features of the electron distribution are discussed in section 3.1, in terms of NAO charges and spin densities obtained by the NBO method.[37] To get a qualitatively correct picture of a singlet diradical in terms of nonzero spin densities, and an energy estimate relevant to a diradicaloid singlet species,[38] the unrestricted DFT (UDFT) monodeterminantal wave function was handled as previously detailed (Supporting Information).[39,30]

Given the well known approximations adopted in estimating free energies, and the further approximation consisting in computing G in correspondence of the transition structures located on the *energy* hypersurface, the actual value of a very small (positive or even negative) ΔG assessed in correspondence of a barrier has a limited meaning. Even more so if this estimate is preceded by the correction to the energy by Yamaguchi's formula,[39] as done in the case of diradicaloid open shells. Small positive or negative estimates are to be intended as an indication of a very easy, or exceedingly easy, reaction step.

A complete set of critical point geometries and energies is presented, together with some relevant spin densities, in the Supporting Information. All molecular calculations were carried out by using the GAUSSIAN03 system of programs.[40]

The periodic LCAO calculations were performed by using the CRYSTAL 2003 program.[41] Structures periodic in one dimension (polymers) can be treated by using Hartree Fock, Density Functional (used here, with the B3LYP functional and the 6-21G(d) basis set)[36b] and hybrid Hamiltonians. The periodicity is fully considered by using cyclic-boundary conditions: the infinite series of coulombic integrals are approximated by Ewald techniques[42] while the infinite exchange series, representing an essentially short range interaction, are truncated while ensuring convergence on the energy and related observables.[43] The solution of the effective one-electron Schroedinger equations is performed in the reciprocal space. The K-points are sampled on a regular mesh: for conducting systems, the Fermi surface is calculated using a denser K-point mesh, using Fourier interpolation of energy bands.[44] The symmetry is fully implemented in the direct space, to minimize the number of molecular integrals to compute and to store, and in the reciprocal space, to perform a block-diagonalization.[45] Recently, energy derivatives with respect to the position of the atoms in the unit cell have been implemented in CRYSTAL, and an automatic optimization of the equilibrium geometry, within a given crystal symmetry, is possible.[46]

3. Results and Discussion

3.1 The molecular and periodic models.

PAHs made by either an odd or even number of carbon atoms (*odd* and *even* PAHs) are also intended here as models to investigate some local features of odd or even soot platelets. Since actual soot platelets could be larger than the molecular models chosen in this study, the computations have been also extended to a periodic representation of a graphene band, which stretches to infinity. Therefore, the periodic computation can be understood as another extreme on the size scale. Both are expected to be helpful to model a soot platelet. If the results of the molecular and periodic models come out to be consistent, the calculations can be deemed sufficiently reliable as regards their ability in describing local chemical features of soot particles.

Structural information about soot and its possibly active surface sites on the atomic scale would be useful in setting up a computational study and in calibrating models: unfortunately this kind of information is very limited. Only a few experimental studies report on this issue to some extent.[47] In setting up some molecular models we have taken into account in particular the ESR results collected by Schurath, Saathoff, and coworkers within the AIDA project for Palas and Diesel soots. They indicate a very low number of ESR active sites on the particle surface, which is of the order of one active carbon out of a number of the order of $n \times 10^3$.[48] Therefore, models containing a large number of vacant valence positions on the edge ("dangling bonds") are more relevant to graphitized carbon particulate, or graphite, than to soot (see for instance refs. 22-26). Consequently, we have chosen to model the local features of odd or even soot platelets by PAHs.

Three even and three odd PAHs have been selected, and O_3 probes their *border* reactivity and functionalization modes. A variety of border positions can be considered. Some of these topological situations[49] can be found in the PAH models chosen here (shown in Chart 1). They have been labeled **Mn** for short, where **n** is the number of carbon atoms. Representative of the *even* class are phenantrene ($C_{14}H_{10}$, **M14**, C_{2v}), anthanthrene ($C_{22}H_{12}$, **M22**, D_{2d}), and coronene, ($C_{24}H_{12}$, **M24**, D_{6h}). Representative of the *odd* class are the phenalenyl radical ($C_{13}H_9$, **M13**, D_{3h}), the fluorenyl radical ($C_{13}H_9$, **M13'**, C_{2v}), and the benzo[*cd*]pyrenyl radical ($C_{19}H_{11}$, **M19**, C_{2v}). Two situations usually considered in the literature are the *zigzag* and *armchair* borders. The former is strictly made by a sequence of *solo* positions, i.e. one secondary carbon, as **b** in **M22** and **M19**, flanked by two tertiary carbons **a** (which are called *fissure sites*).[49] The latter is instead defined by alternating *duo* groups (a couple of secondary **c** atoms taken in between two tertiary **a** atoms, as in **M22** or

M24) and *bay* regions (as the sequence **caac** in **M14** and **M13'**). A *trio* position is recognizable in **M22**, **M13,** and **M19**, as the sequence **cdc**. Among these positions, we have considered in the following those giving origin to the stablest intermediates.

CHART 1: Even molecular models (top): phenanthrene (**M14**), anthanthrene (**M22**), and coronene (**M24**). **Odd molecular models** (bottom): the phenalenyl radical (**M13**), the fluorenyl radical (**M13'**), and the benzo[*cd*]pyrenyl radical (**M19**). All are shown by a single resonance structure. Letters label peripheral positions following this convention: **a** = tertiary carbons, **b** = secondary carbons between two tertiary carbons; **c** = secondary carbons between a tertiary carbon and a secondary carbon; **d** = secondary carbons between two secondary carbons.

Ozone is an electrophilic molecule and should be attracted by the highest electron density positions. In the even systems, these are, for coronene (**M24**), those on the secondary carbons along the perimeter (**c**, *duo* positions), and for anthanthrene (**M22**) chiefly the *solo* (**b**) position, followed by the *duo* (**c**) position (see the NAO charges[37] shown in Chart 2). Fissure sites (tertiary carbons along the borders) are relatively depleted of electron density. The *trio* group in **M22** (**cdc**, locally resembling an allyl system) exhibits intermediate values on its terminal sites **c**.

CHART 2: Even models (upper line): NAO charges on border carbons (CH group charges in parentheses) for phenanthrene (**M22**), anthanthrene (**M22**) and coronene (**M24**). **Odd models** (lower line): NAO spin densities (italic) on border carbons for the phenalenyl radical (**M13**), the fluorenyl radical (**M13'**), and the benzo[*cd*]pyrenyl radical (**M19**).

Ozone, though an even electron system, is also sensitive to high spin density positions in odd systems (Chart 2), as discussed in our preceding paper.[32] NAO integrated spin density $\Delta\rho$ ($\Delta\rho = \rho^{\alpha} - \rho^{\beta}$, excess α electron population over β)[37] reveals itself as spin waves (Supporting Information), i.e. the spin density positive values alternate with negative values, which are generally lower in absolute value (an exception is **M13'**, which has the unpaired electron localized on the *solo* positions, as shown in Chart 1).[50] PAH systems with one unpaired electron show several integrated atomic spin density population with significant values, up to more than 0.5 electrons. Higher spin density values are generally found on some peripheral positions than on internal positions. In particular, the highest values are in correspondence of *solo* positions. For a *trio* site (**c**, **d**, **c** in Chart 1), the spin density is higher on the locally terminal positions, thus resembling the situation found in an allyl radical. If the system is attacked by a species sensitive to the $\Delta\rho$ variable, it is reasonable to assume that the attack will be more easily carried out on some perimeter sites. The integrated $\Delta\rho$ proves

to be a quantity rather insensitive to a change in optimized geometry and basis set (see ref 32).

Similar definitions apply to the periodic models shown in Chart 3. The closed shell models **P1** and **P2** have singlet spin multiplicity in the elementary cell, while the open shell model **P3** has doublet spin multiplicity in the elementary cell.

CHART 3: Periodic models. Arrows indicate the adopted elementary cells. Letters label peripheral positions mentioned in the text.

3.2 The possible pathways.

Free energy difference estimates ($\Delta G^{\ddagger}$ and ΔG, in kcal mol^{-1}) will be discussed in the following. More complete energetics can be found in the Supporting Information. The conceivable reaction pathways for ozone addition are sketched in Scheme 1, for an even system (symbolically represented by a single aromatic ring), and in Scheme 2, for an odd system (focusing again on a single aromatic ring). As in the preceding papers, dealing with internal positions,[29,32] acronyms label intermediates and transition structures which connect them.

SCHEME 1. Even systems. Conceivable pathways explored for the molecules in Chart 1 (symbolically represented by a single 6-membered ring).

SCHEME 2. Odd systems. Conceivable pathways explored for the molecules in Chart 1 (the scheme focuses on a single 6-membered ring).

The addition to the unsaturated system, starting from the reactants R, can take place in principle either by a concerted process (in which the two C–O bonds form in a more or less synchronous way), or by a two-step process, with initial formation of a single C–O bond. A concerted attack (left side of Schemes 1 and 2) would lead directly to the primary ozonide intermediate (PO, with a local 1,2,3-trioxolane structure). For an even PAH, the initial PO is a closed shell molecule; for an odd PAH, the π-delocalized PO is instead a π radical (which we could dub "π·PO"), because it obviously maintains an odd number of π electrons. The two-step pathway (right side of Schemes 1 and 2) produces first, in the case of an even PAH, an open-chain trioxyl diradical, TD. In an odd PAH, an open-chain trioxyl radical, TR, would be produced istead, with a closed-shell π system on the "PAH part".

We discuss in the next subsections the evolution of the even and odd polycyclic systems (Chart 1). Then, some processes, possibly competitive with ozonization, which could alter

the substrate nature (O_2 addition or radical coupling in odd systems; radical attack on even systems) are discussed.

3.3 Even systems.

Initial attacks. All sites (*solo*, **b**; *duo*, **cc**; *trio*, **cdc**) are available in **M22**, while only the *duo* position is present in **M24.** In the case of **M14**, only the *bay* position (**caac**) is considered. The energetics (relevant to all models) is reported in Table 1, for the initial steps to PO and TD. In the text reference is made to the free energy differences, relative to the separate reactants. The G profiles are displayed in Figure 1a (Figure 1b reports similar data for the odd systems, displayed together to allow an easier comparison).

TABLE 1. Energy and Free energy differences[a] for the initial O_3 attacks on even PAH systems[b].

Model/position:	M22 / solo		M22 / duo		M24 / duo		M14 / bay 1,4		M14 / bay 1,2	
Structure[c]	ΔE	ΔG	ΔE	ΔG	ΔE	ΔG	ΔE	ΔG	ΔE	ΔG
TS R-PO	10.5	23.6	9.7	23.3	12.9	26.3	*36.6*[d]	*49.5*[d]	20.3	33.9
PO	-14.3	1.7	-32.5	-16.1	-25.6	-9.6	10.9	27.2	-0.1	15.6
TS R-TD	0.6	12.6	5.4	17.4	8.9	20.8		8.8	21.1	
TD	-7.8	4.1	2.6	14.2	7.4	18.9		6.3	18.5	
TS TD-PO	-4.2	10.0	0.0	13.5	5.3	18.7	20.3	34.3	11.8	25.6

[a] kcal mol^{-1}; T=298 K; reference: the separate reactants.
[b] see Chart 1, top.
[c] see Scheme 1.
[d] a second order saddle point.

FIGURE 1. Free energy profiles for the initial O_3 attacks on (a) closed shell and (b) open shell PAH systems. The lines for **M13** and **M19** *trio* result superimposed. *Trio* and *solo* curves: dashes indicate portions of the *E* surface where an all-downhill steep reaction pathway is found (*G* not determined).

Some features are qualitatively shared by the *solo* and *duo* positions (not always by the **M14** 1,4 *bay* case, discussed apart; see below). PO is stabler than TD in all cases, and the energy difference is more significant for the *duo* positions. However, the stability differences are contrasted by the free energy barriers, that describe always TD formation as easier than

PO formation. Moreover, all barriers for the TD to PO conversion are well below the barriers for direct PO formation. Therefore, in any case PO is likely to form through TD. For the *duo* positions the step is exceedingly easy, to the point of questioning the very existence of TD as intermediate.

Coming now to the *bay* positions in **M14**, we see that these (**caac**, Chart 1), alternate with *duo* groups (**acca**), and both are representative of armchair borders. Different attack modes are conceivable, involving in particular 1,2 (**ca**) or 1,4 (**cc**) positions. Though PO corresponds in any case to an energy minimum, it is not a very stable structure, in particular for the 1,4 attack, if compared to the preceding data. The results collected[51] rule out any concerted attack on a bay region. The alternative formation of TD presents lower barriers, which, together with TD stability, are closer to the *duo* data than the corresponding PO results. As a last trait, the TD-PO conversions present more sizeable barriers, compare to those seen for the *solo* and *duo* cases, and consequently we feel that any role of PO can be ruled out.

Some possible further transformations of PO and TD will be now discussed (making reference to the step labels of the intermediates in Scheme 1).

Further steps from the primary ozonide.

The PO relevant to a *solo* position (**M22**) was shown to be relatively stable and also reachable in principle through a TD pathway, with a barrier for the step TD-PO of 6 kcal mol^{-1}. However, since it will be shown in the following subsection that TD prefers to evolve differently, further *solo* PO evolutions are not considered here.

We have seen that PO is particularly stable for *duo* groups, in which case it is reachable through a TD-pathway, i.e. a presumably concerted but highly asynchronous addition. Its possible further transformations are discussed here only for **M24**. The energetics is reported in Table 2.

The cleavage of any of the three kind of bonds of the PO trioxolane ring can be possible. (1) The C–O cleavage (interconversion PO-TD) has already been considered. (2) Alternatively, O–O bond cleavage gives a singlet peroxyl oxyl diradical, ^{1}POD. But the backwards step from ^{1}POD to PO is estimated to be barrierless, while the fragmentation modes of POD are found to imply sizable free energy barriers.[52] So, the PO-POD step corresponds to a dead-end pathway. (3) When studying the third possibility, C–C bond cleavage in the trioxolane ring of PO, one finds that it is concerted with one O–O bond cleavage and with the closure of a dioxirane ring, in other words concerted with the formation of one new C–O σ bond and with the π bond of a carbonyl group (see sketch below; new bonds indicated by dashed arrows).

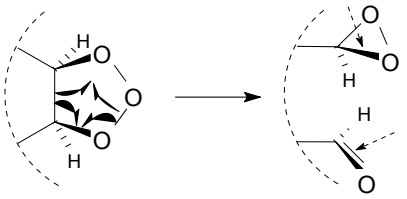

TABLE 2. Energy and free energy differences[a] for the steps originating from PO in the M24 model system (*duo* group).[b]

(Path) structure	ΔE	ΔG
Steps from PO: [c]		
PO	-25.6	-9.6
TS PO-^{1}POD	-11.8	3.1
^{1}POD	-10.0	3.9
TS ^{1}POD-^{3}OD	7.0	17.6
TS PO-AD	-8.3	6.3
AD	-40.3	-27.0
Evolutions of AD: [d]		
(a) TS AD-AL	54.3	62.9
AL	-132.1	-129.5
(b) TS AD-EPA	-28.4	-15.7
EPA	-63.4	-49.3
(c) TS AD-PL	-3.9	9.7
PL	-68.5	-52.7
TS PL-LA	-17.4	-4.5
LA + H_2CO	-132.5	-131.7
TS PL-PY	-34.6	-21.9
PY + CO_2	-140.8	-136.0
(d) TS AD-DA	-18.5	5.2
DA + 2 $^3O_2$	-110.0	-108.1

[a] kcal mol^{-1}; T=298 K; reference: the separate reactants.
[b] see Chart 1, left.

This step requires surmounting a barrier slightly above the reference level, yet significantly lower than that overcome initially by the two reactants (ca. 21 kcal mol^{-1}). The intermediate thus formed is an “aldehyde dioxirane” (AD) open chain system, positioned well below PO (Figure 2) and the step is irreversible.

FIGURE 2. Free energy profiles for PO evolutions of in **M24** (*duo* position).

Since AD formation, though presumably slow, presents these traits, we decided to explore possible further steps stemming from this intermediate [see the (a)-(d) paragraphs below and Scheme 3].

SCHEME 3. Further steps from AD in **M24** (which is shown only partially, dashed contour).

(a) A first exploration actually provides a negative information. A TS AD-AL, concerted with H migration from the dioxirane ring and leaving an aldehyde plus carbon dioxide, could in fact be identified, but the step presents too high a barrier above AD.

(b) Through O–O bond cleavage concerted with two C–O bonds formations in AD, two new condensed ether rings can form (see sketch below; new σ bonds indicated by dashed arrows).

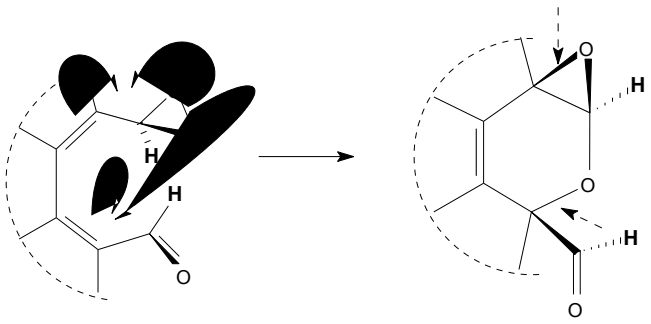

A polyfunctional intermediate is obtained, which we could dub “epoxy pyran aldehyde” (EPA), since one ring is an epoxide function, while the other recalls the structure of 2-*H*-5,6-dihydropyran.This step, that requires to overcome a barrier from AD which is well below R, is significantly exoergic and irreversible. Therefore, the hardest step to get this border functionalization is the previous formation of AD from PO, more likely in a low-pressure experiment than at tropospheric pressure.

(c) Through O–O bond cleavage in AD, concerted with another O–O bond formation, a “peroxy lactone” intermediate could form (PL). The step is very exoergic, but the relevant barrier is almost 10 kcal mol^{-1} above R. Though the step can appear not very easy, its barrier is again lower than that overcome initially to get PO, and the overall process is unimolecular. If PL had a chance to form, e.g. in low pressure experiments, it could further

produce either formaldehyde together with a lactone (LA in Scheme 3; compare ref 18c), or carbon dioxide[16,53] and a pyrane ring (PY).

(d) As a final point, attack of a second O_3 molecule onto the dioxirane ring of AD, can give a dialdehyde (DA, see below the sketch depicting the relevant process). In experimental studies of PAH ozonization this kind of functionalization, as well as lactone and ketone functionalities, were observed.[18]

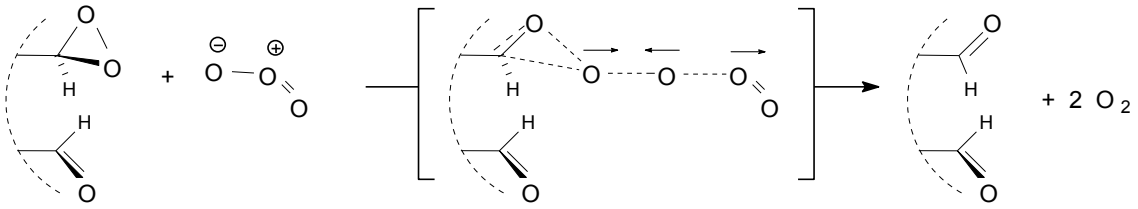

Though this step would be very exoergic, TS AD-DA is 5 kcal mol^{-1} above R. Since this time the step is bimolecular it is also much more problematic, and the channel could be considered only in experiments involving high ozone concentrations.

In concluding this subsection, we can observe that PO could play some role in the *duo* position of even systems, and give way to the formation of polyfunctional oxidized regions of the PAH or soot platelet (ether bonds, aldehydic groups, etc.). When the steps require to overcome barriers close to the reference level defined by the separate reactants, one can deem them as unfeasible if thermalization at tropospheric pressures is assumed (more so if the step is bimolecular or involving particles), yet some could be taken into account if gas phase low-pressure experiments were carried out on PAHs. Finally, in some experimental papers room temperature production of CO_2 from soot in the presence of ozone was detected.[16,53] Though our models represent a very simplified situation, we tried to assess if structures as those just discussed could be possible candidates for CO_2 loss from a region of a soot platelet. The conclusion is that CO_2 production from soot is more likely to occur from different functionalities (possibly bound to aliphatic chains).

Further steps from the trioxyl diradical.

The energetics relevant to the evolution of the initial TD intermediates (Scheme 1) are collected in Table 3 and displayed in Figure 3 for the *solo* position in **M22** and the *duo* position in **M24**. In the case of a *bay* position, TD would play just the same role as for the *duo* positions and consequently will not be discussed as a separate case.

FIGURE 3. Free energy profiles for the further evolutions of TD in even PAH systems: (a) **M22** (*solo* position) and (b) **M24** (*duo* position).

TABLE 3. Energy and free energy differences[a] for the TD evolutions in the closed shell M22 ad M24 model systems.[b]

Model/position:	**M22 / *solo***		**M24 / *duo***	
structure	ΔE	ΔG	ΔE	ΔG
(a) ^{1}TD	-7.8	(4.1)	7.4	(18.9)
TS ^{1}TD-^{1}HT	-6.8	(6.2)	8.8	(21.1)
^{1}HT	-38.2	(-24.4)	-37.1	(-23.5)
TS ^{1}HT-$\pi^{\bullet}$KE	-38.2	(-25.4)	-38.9	(-26.4)
$\pi^{\bullet}$KE +HOO	-62.6	(-56.1)	-42.4	(-43.2)
(b) TS ^{1}TD-^{3}OD	-6.4	(4.8)	10.4	(20.1)
^{3}OD + $^3O_2$	-11.7	(-11.9)	4.3	(3.6)
^{3}EPO + $^3O_2$		—[c]	7.0	(6.2)
TS ^{3}OD-^{3}PH	-11.1	-12.1	4.5	(3.3)
^{3}PH	-39.8	-40.9	-13.5	(-15.6)
TS ^{3}OD-^{3}KE	5.3	1.6)	5.7	(4.1)
^{3}KE	-25.9	-26.6	-23.6	(-25.3)
^{3}TD	-8.1	3.4	—[d]	
TS EPO-OX	5.8	7.6	—[e]	
TS ^{3}TD-^{1}EPO	-7.0	3.6	—[d]	
^{1}EPO + $^3O_2$	-34.2	-31.8	-40.2	-37.6

[a] kcal mol^{-1}; T=298 K; reference: the separate reactants.
[b] see Chart 1, left. [c]unstable, it spontaneously opens to OD.
[c] unstable, it spontaneously opens to ^{3}OD.
[d] unstable, it spontaneously loses O_2.
[e] OX unstable.

***Solo* position (M22).** In the singlet trioxyl diradical one electron is localized on the terminal oxygen atom, while the other is π-delocalized. Three alternative and easy transformations of ^{1}TD can take place, to be compared with the transformation TD-PO.

(a) Along the path ^{1}TD-^{1}HT-^{2}π·KE, rotation along the CO–OO· dihedral angle (dashed arrow in the sketch below, where an oval stays for the PAH-like part of the intermediate) from the stablest anti conformation to the hypothetical syn, comes out to be concerted with the abstraction of the H geminal to the rotating group. The barrier is very low, and lower that the TD-PO barrier. This step easily leads to the hydrotrioxyl (^{1}HT) intermediate, well below ^{1}TD, which then loses also very easily HOO· with an estimated nul G barrier, though for even systems ^{1}HT exists as a well defined minimum on the E hypersurface.

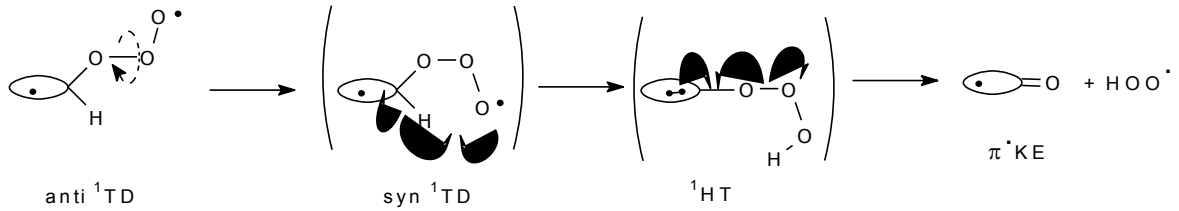

The product of this significantly exoergic channel is a ketone having one π unpaired electron, π·KE. The overall transformation TD → π·KE appears to be a concerted asynchronous process, and is very exoergic. It is interesting to note that, by the reaction steps R →TD (→ HT) → π·KE, an even π system has turned into an odd one.

(b) A second, and even easier, transformation of ^{1}TD is $^3O_2$ loss. Through this exoergic step, a triplet oxyl diradical forms with conservation of the overall spin multiplicity (^{3}OD). The ^{1}TD-^{3}OD TS is related to a very modest barrier, lower that the TD-PO barrier. ^{3}OD is positioned well below ^{1}TD. ^{3}OD could have a hypothetical isomer, ^{3}EPO, with triplet multiplicity associated to the π system, but this structure is not stable and opens spontaneously to give ^{3}OD (not shown in Scheme 1).[54] Let us now examine, along this pathway, how ^{3}OD can evolve. If an inter-system crossing (ISC) had a chance to occur in ^{3}OD, ^{1}EPO would form directly, since ^{1}OD (in parenthesis in Scheme 1) is not stable. In ^{3}OD, migration of the H_{gem} to the oxygen atom can take place and produce a triplet phenol ^{3}PH, in a very exoergic step. For the relevant TS ^{3}OD-^{3}PH a nul barrier with respect to ^{3}OD is estimated. An alternative migration of H_{gem} toward the carbon adjacent to the oxyl group generates, this time with a non-negligible G barrier with respect to ^{3}OD (yet located below ^{1}TD), a triplet ketone, ^{3}KE, located well below ^{1}TD. This last step is somewhat more demanding than the preceding ones. Figure 3a illustrates these features.

^{1}EPO could also form after a possible ^{1}TD-^{3}TD ISC. ^{3}TD (which is actually slightly stabler than ^{1}TD, by less than 1 kcal mol^{-1}) could in fact undergo an almost barrierless $^3O_2$ loss. This step would generate an epoxide ^{1}EPO, located well below ^{3}TD. In TS ^{3}TD-^{1}EPO the asynchronous O–O bond cleavage is concerted with the epoxide ring closure.

Since the ^{1}TD transformations just discussed can take place more easily than its conversion to PO, for the attack onto the most reactive *solo* position PO can have a limited role.

***Duo* group (M24).** In this case, ^{1}TD is higher than for the *solo* position and well above PO. Let us also recall that the transformation of TD to PO is extremely easy. Figure 3 (in which the two TD intermediates are set as the reference) allows us to easily notice further differences, and similarities, between the *solo* and *duo* cases. (a) Also here, the very exoergic sequence R $\rightarrow$TD ($\rightarrow$ HT) $\rightarrow$ π·KE (which turns an even π system to an odd one) presents a very low TD-HT barrier followed by a barrierless HOO· loss. (b) Alternatively, $^3O_2$ loss from ^{1}TD can occur also in this case, to give ^{3}OD (barrier almost as high as for *solo*). However, these steps could be seen as somewhat less easy than the transformation of TD to PO.

Further remarkably easy steps from ^{3}OD could produce either a triplet phenol (^{3}PH) or a triplet ketone (^{3}KE) in similarly easy and quite exoergic steps. ^{3}KE formation would be much easier for the *duo* case than was for the *solo*. However, for this position, the very formation of ^{3}OD from ^{1}TD might appear dubious in a thermalized system. These step could instead have a chance to occur if a gas phase low-pressure experiment on PAHs were carried out. ^{3}OD, if formed, could possibly undergo ISC: in this case, since ^{1}OD is not a stable intermediate, spontaneous ring closure to ^{1}EPO would take place. ^{3}EPO, on the other hand, which could as well accompany $^3O_2$ loss with spin conservation, is stable in this case, at variance with the *solo* position.[55] The stablest dissociation limit is of course ^{1}EPO + $^3O_2$: if an intersystem crossing ^{1}TD $\rightarrow$ ^{3}TD had a chance to occur, it would actually lead directly to it, since ^{3}TD, at variance with the solo case, is not a minimum on the energy hypersurface, and loses $^3O_2$ spontaneously. This way, the overall process would be: ^{1}TD (ISC)—[^{3}TD]$\rightarrow$^{1}EPO + $^3O_2$.

In summary, for even systems, ozone attack to *solo* (zigzag) positions is significantly easier than to *duo* (armchair) groups, and takes place through a TD pathway. Though PO is stabler than TD in all cases, particularly for *duo* positions, it could probably form only by passing through TD rather than directly from the reactants. For the most reactive *solo* position, no PO pathways can be important, since the TD-PO conversion is contrasted by some easier transformations stemming from TD itself, illustrated in Figure 3, which bring

about the formation of epoxidic, phenolic, or ketonic functionalities. This situation is different in the less reactive *duo* positions. *Duo* TD is higher in energy than *solo* TD, though it forms again more easily from reactants than PO. However, the TD-PO interconversion is in this case quite easy, and probably both pathways, through TD and through PO, are viable.

3.4 Odd systems.

Initial attacks. The energetics is reported in Table 4, for the initial steps to PO and TR. The features of the initial O_3 attack onto odd systems are summarized in Figure 1b (and can be compared to those displayed in Figure 1a for even systems).

TABLE 4. Energy and free energy differences[a] for the initial O_3 attacks on open shell PAH systems[b] with an odd number of unsaturated carbon atoms and π electrons.

Model/position:	M19 / solo		M19 / duo		M19 / trio		M13 / trio (1,2 attack)		M13'/ bay (1,4 attack)	
Structure[c]	ΔE	ΔG	ΔE	ΔG	ΔE	ΔG	ΔE	ΔG	ΔE	ΔG
π·-PO	-8.3	7.4	-27.7	-11.4	-20.3	-4.4	-21.5	-5.6	3.1	19.0
TS R-TR	—[d]		5.6	17.7	—[d]		—[d]		17.6	29.2
TR	-27.8	-13.9	-8.5	4.8	-21.6	-8.1	-22.4	-8.8	4.4	16.7
TS TR-PO	-5.2	9.9	-1.4	12.9	-7.3	7.7	-8.4	6.7	20.6	4.9

[a] kcal mol^{-1}; T=298 K; reference: the separate reactants.
[b] see Chart 1, bottom.
[c] see Scheme 2.
[d] The R to TR transformation corresponds to portions of the *E* surface where an all-downhill steep reaction pathway is found, and *G* is not determined.

All sites (*solo*, *duo*, or *trio*) are available in **M19**, while only the *trio* position is present in **M13.** In the case of **M13'**, only the bay position is considered. In all cases, the formation of ^{2}TR comes out to be significantly more exoergic than was for TD in the case of even PAHs. Though a PO minimum exists on the energy hypersurface (at higher energy than R), we find that, at variance with the even systems, there is indication that the concerted PO-like saddle point is not first order, i.e. it does not correspond to a transition structure (Supporting Information). However, an interconversion TS TR-PO can be found.

The *solo* position in **M19** and the *trio* group in both **M19** and **M13** share some similar traits. All see a formation of a trioxyl radical ^{2}TR stabler than R (in the *duo* case ^{2}TR is located higher than R). Though the two *trio* positions in **M19** are not equivalent, the

corresponding trioxyl radicals are found to be nearly as stable (in Table 3 are reported the data for position **c**).[56] TR formation takes place along a pathway on the *E* surface from the reactants that is all-downhill. In the *duo* case, the rather stable PO could be easily attained from ^{2}TR, by closing a bond in **d**, but non-concerted ozone addition to the *duo* position is not competitive with additions on *solo* and *trio* positions, since it requires overcoming a G barrier.

The *bay* position in **M13'** has different features. PO, coming from a 1,4 attack, is found as a relatively high-free energy minimum, and does not appear to be an interesting intermediate. The two-step O_3 addition to the **c** positions in **M13'** is not competitive with additions to the positions just discussed above. Compared to these situations, also TR is rather high above R. So, the overall ozone attack scenario on a bay group is not promising.

Further evolutions. We will now discuss some possible transformations of the TR intermediate, generated from ozone attack to armchair borders of **M13** (trio position) and **M19** (solo and trio positions), (see Scheme 2). The energetics of the evolution from the initial intermediates are collected in Table 5.

TABLE 5. Energy and free energy differences[a] for the TR evolutions in the open shell M13 ad M19 model systems.[b]

Model/position:	**M13 / *trio***		**M19 / *solo***		**M19 / *trio***	
Structure[c]	ΔE	ΔG	ΔE	ΔG	ΔE	ΔG
^{2}TR	-22.4	-8.8	-27.8	-13.9	-21.6	-8.1
TS ^{2}TR-^{2}KE	-27.1	-14.2	-26.8	-11.9	-24.4	-11.4
^{2}KE + HOO	-66.3	-66.4	-72.4	-70.3	-65.8	-64.0
TS ^{2}TR-^{2}EPO	-23.8	-11.3	-29.2	-16.2	-23.0	-10.6
^{2}EPO + $^3O_2$	-35.7	33.2	-28.7	-26.5	-34.4	-32.0
TS ^{2}EPO-^{2}OX	-20.9	-19.8	-19.3	-17.8	-20.6	-19.5
^{2}OX + $^3O_2$	-35.9	-33.7	-33.2	-32.3	-36.3	-34.0
TS ^{2}EPO-^{2}OR	-19.0	-17.3	-26.5	-24.6	-24.4	-22.4
^{2}OR + $^3O_2$	-26.4	-24.9	-32.7	-30.9	-25.7	-24.2
TS ^{2}OR-^{2}RP	-11.4	12.0	-16.0	-16.2	-11.1	-11.8
^{2}RP	-72.0	-69.4	-70.9	-68.7	-70.7	-68.9
TS ^{2}OR-^{2}RK	-17.3	-18.1	-19.8	-20.7	-4.6	-6.2
^{2}RK	-63.1	-61.8	-49.3	-47.5	-62.6	-61.2

[a] kcal mol^{-1}; T=298 K; reference: the separate reactants.
[b] see Chart 1, bottom.
[c] see Scheme 2.

As for even systems, the primary ozonide and trioxyl intermediate can in principle interconvert (Scheme 2). Formation of $\pi^{\cdot}$-^{2}PO from ^{2}TR requires overcoming *G* barriers of 24-16 kcal mol^{-1} (Table 4). However, as we will presently see, exceedingly easy steps from ^{2}TR are shown to rule out the ozonide and any channel involving its intermediacy.

The possible evolutions of ^{2}TR would depend on processes already examined for the even PAHs. One could be intramolecular H abstraction/HOO loss, with formation of a closed shell ketone, KE. Alternatively, $^3O_2$ loss could either give an oxyl radical, ^{2}OR, or an epoxide having one unpaired electron in the π system, $\pi^{\cdot}$-^{2}EPO. These could interconvert. An epoxide -oxepine (OX) interconversion could as well be viable. ^{2}OR could subsequently produce a radical phenol, ^{2}RP, or a radical ketone, ^{2}RK, via 1,2 *gem*-hydrogen shifts to the oxygen, or to the adjacent carbon respectively.

FIGURE 4. Free energy profiles for the further evolutions of TR in the open shell PAH system **M19** (*solo*, **a**, and *trio*, **b**, positions).

Only the *anti* conformer of ^{2}TR can be found as a minimum energy point. A first order *gauche* saddle point related to rotation along the CO–OO dihedral angle would lead toward to the *syn* conformer. But this does not exist as a stable structure, because rotation triggers a spontaneous HOO$^{\cdot}$ loss (dashed arrow in the sketch below). The step is characterized by H_{gem} abstraction by the terminal –O$^{\cdot}$, concerted with O–O bond cleavage. These events take place in an asynchronous way and the hydrotrioxyl cannot be found.

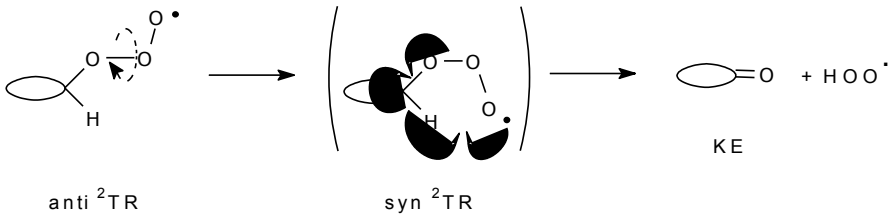

The G barrier is assessed as negative with respect to ^{2}TR for all three situations. This result alone would rule out any role of $\pi^{\cdot}$-^{2}PO. The product of this HOO$^{\cdot}$ loss is a ketone, KE, located in all cases well below ^{2}TR. An odd system has thus turned into an even one.

As regards the alternative $^3O_2$ loss from ^{2}TR, this could leave in principle an oxyl radical, but we have indications that ^{2}OR cannot form directly. $^3O_2$ loss from ^{2}TR is found instead concerted with ring closure, and gives a π radical epoxide, $\pi^{\cdot}$EPO. No barrier is present for this step. Also this result concurs to exclude the intervention of the primary ozonide. The intermediate $\pi^{\cdot}$-EPO lies below ^{2}TR. The epoxidic ring can subsequently open to give the oxyl radical, ^{2}OR. The EPO-OR barrier is significantly lower for **M19** *solo*. A transformation of $\pi^{\cdot}$-EPO to its other isomer, oxepine, is also possible.

The next steps concern two possible unimolecular transformations of ^{2}OR. Both present barriers higher than the ^{2}EPO minimum, but close to the ^{2}TR intermediate free energy, and are very exoergic steps (Figure 4). A 1,2 H_{gem} shift to the radical oxygen brings about the formation of a radical phenol ^{2}RP, in which the unpaired electron belongs to the π system. This $\pi^{\bullet 2}$RP forms overcoming a barrier lower to some extent than the ^{2}TR intermediate, and is located significantly below ^{2}TR. A 1,2 H_{gem} shift to the radical oxygen leads instead to the formation of a radical ketone (^{2}RK). The barriers are not very different from those leading to ^{2}RP, and both channels appear viable.

In concluding this subsection on odd PAHs or soot platelets we can remark that an ozone attack on *solo* and *trio* positions is particularly easy (an all downhill pathway on the *E* surface). PO cannot form directly from reactants, in odd systems and, though reachable in principle through an ensuing TR-PO conversion step, plays no role at all, since different transformations of TR are much easier. In these first attacks, PO is stabler than TR only for the relatively unreactive *duo* positions, and is less stable for the more reactive *solo* and *trio* positions.

3.5 Possibly competitive processes.

For the odd systems, some processes which in principle could be in competition with ozone addition, and alter the substrate nature, have been considered: (1) dioxygen addition, (2) radical coupling, and (3) radical attack on closed shell species (Table 6).

TABLE 6. Energy and Free energy differences[a] for some hypothetically competitive processes.

additions:	**M13** + O_2		**M13** + **M13**		**M13** + **M16** position 1		**M13** + **M16** position 4	
Structure	ΔE	ΔG	ΔE	ΔG	ΔE	ΔG	ΔE	ΔG
TS	8.7	20.7	10.1	25.8	28.8	41.9	28.6	44.1
intermediate	5.3	18.1	1.2	18.5	23.5	37.4	21.1	40.3

[a]kcal mol^{-1}; T=298 K. Reference: the separate reactants.

(1) Dioxygen attack onto some perimeter, high $\Delta\rho$, position of an odd PAH or soot platelet could destroy its characteristics, because the odd substrate would become an even π-system, decorated on its perimeter by a peroxyl radical group. To estimate how easy can this attack be, we have studied the **M13** + O_2 radical coupling. In the "allylic" positions **a**, involving the highest spin density carbon atom (Chart 1), the peroxyl radical is stable.[57] The

barrier for its formation is rather high, and the addition step is endoergic. These values have to be matched up to the remarkably easy ozone attack and indicate there is no competition between the two radical electrophilic additions, notwithstanding the higher concentration of O_2. (2) The coupling of two odd systems has then been modeled (though it seems rather unlikely right from the onset) by the dimerization of **M13**, involving again the highest spin density **a** positions. The reaction is quite endoergic in terms of G, and the coupling barrier is sizeable. This process is therefore to be discarded. (3) Even less easy is the attack of an odd system onto an even system, exemplified by the additions of **M13** to pyrene, **M16**, positions 1 or 4. These additions require to overcome similar barriers, quite high in terms of *G*. The reactions are significantly endoergic. Also this kind of process cannot compete with ozone addition.

Thus, all have been found not competitive.

3.6 Periodic calculations.

We have calculated on periodic models the thermochemistry of some reactions, to verifiy the possible presence of solid state "long range" effects, potentially relevant in these cases, due to the electron delocalization in polyaromatic systems. The models, periodic in one dimension, are displayed in Chart 3. They are infinite flat ribbons, having even (P1, P2) or odd (P3) number of electrons per unit cell, and zigzag (P1, P3) or armchair (P2) borders. The polyaromatic ribbons are here used as models of the border of very large poly-aromatic platelets. Recently polyaromatic nano-ribbons have been studied both theoretically and experimentally due to their properties and applications in materials sciences and molecular electronics.[58]

In Table 7 the reaction energies of the periodic models with ozone giving ketone and epoxide product are reported, together with the reaction energies of the corresponding molecular models. P1 *solo* should be compared with **M22** *solo*, P2 *duo* with **M24** *duo*, P3 solo with **M19** *solo*, and finally P3 *trio* with **M13** and **M19** *trio*. Table 7 shows a qualitative correspondence between molecular and periodic models.

TABLE 7. Energy differences[a] for the periodic models.[b]

Model/position: Structure	**P1 / *solo***	**P2 / *duo***	**P3 / *solo***	**P3 / *trio***
	ΔE			
KE + $^3O_2$	-43.2	-36.6	-69.5	-39.2
EPO + $^3O_2$	-32.2	-38.7	-26.8	-34.4

[a] kcal mol^{-1}; T=298 K; reference: the separate reactants.

[b] see Chart 3.

If the molecular models adopted in this study give a correct picture of the reactivity of large polyaromatic platelets, the periodic models show the same landscape, demonstrating that there are not "solid state effects" in the reactivity.

4. Conclusions

The following general comments can be drawn. By comparing the present results to our previous work on ozonization of internal sites of even and odd models, we find that some border positions are more reactive than internal positions. In all models, the most reactive perimetral positions are of zigzag type, which have been found to allow easier ozone addition in odd systems (*solo*, *trio* positions) than in even systems (*solo* position). Ozone can add either in a concerted way, with formation of a primary ozonide PO, or in a non-concerted manner, with formation of a trioxyl intermediate (TD or TR). Additions to *solo* or *trio* positions are preferentially non-concerted. If attacks to the less reactive armchair type border zones (*duo* or *bay* positions) were possible, these would be again non-concerted, but, for even systems, PO could very easily form by passing through a “trioxyl intermediate-type” pathway (the real presence of such an intermediate is in this case dubious).

Some more detailed information is summarized in the following.

Even systems. From reactants R a trioxyl diradical TD is formed more easily than PO, though PO is stabler than TD in most cases (particularly for *duo*). So PO is indicated to form only by passing through TD, rather than directly from R. In the most reactive *solo* position, the TD-PO conversion is contrasted by some easier transformations stemming from TD itself, in such a way that PO can conclusively be ruled out. By contrast, for the less reactive *duo* positions, if they had a chance to be attacked, the TD-PO interconversion is exceedingly easy, as said above, and PO could play some role. In any case, the TD-*solo* and PO-*duo* pathways give way to the formation of polyfunctionally oxidized regions of the PAH or soot platelet. Namely: (1) from TD-*solo*: epoxy, phenol, ketonic groups, with dioxygen production; or, as an alternative, a radical ketone could form, with hydroperoxyl radical formation (this would be notable, since it would turn an even system into an odd one); (2) from PO-*duo*: an ether group (with CO_2 loss), possibly two aldehydic groups (with O_2 loss), or possibly a lactone group (with H_2CO loss); or, as an alternative easier than the preceding ones, epoxy, ether, and aldehydic groups, all concurrently formed to give a polyfunctional site.

Odd systems. The attack on the more reactive *solo* and *trio* positions, which gives a trioxyl radical TR, is presumably barrierless or having a low barrier, while a PO-like pathway

does not exist altogether. Since further transformations of TR are much easier than its conversion to PO, PO plays no role at all. The functionalization achieved through a TR pathway leads again to an epoxidic group, or to radical phenol or radical ketone groups (with concurret dioxygen formation). A closed shell ketone plus hydrotrioxyl radical could also form, this time turning an odd system into an even one. This can be compared with the outcome of experimental studied on PAH ozonization.[17,18]

We conclude that border functionalization, regardless of how achieved, gives largely the same functional groups, most of which actually observed in experimental studies on PAH ozonization. Some of the functionalizations are accompanied by dioxygen production: this was actually observed in some experimental investigations.[14,15,16] This can be compared with our previous results on internal sites, for which epoxidation was the only outcome. Though the study of further evolutions of the oxidized products is beyond the scope of this study, we like to point out that one of these processes, most interestingly, is able to turn an even system into an odd one, and conversely.

Acknowledgment. This work was conducted in the frame of EC FP6 NoE ACCENT (Atmospheric Composition Change, the European NeTwork of Excellence) and supported by a grant from Regione Piemonte [DDn.1 18.1.2006; DD.n. 64 2.12.2005; Bando Ricerca Scientifica - Settore Sviluppo Sostenibile]. A.G.'s bursary was also provided by Regione Piemonte.

Supporting Information Available: The Supporting Information includes the geometries of all optimized structures, the corresponding total energies, and some information about electron distribution and spin densities. This material is available free of charge via the Internet at http://pubs.acs.org.

References and Notes

[1] Raes, F.; Van Dingenen, R.; Vignati, E.; Wilson, J.; Putaud, J.-P.; Seinfeld, J. H.; Adams P. *Atmos. Environ.* **2000**, *34*, 4215-4240.

[2] A crystalline structure is defined as *turbostratic* when the basal planes are moved sideways relative to each other, bringing about a larger inter-plane distance with respect to a regular structure. If we compare soot to graphite, this irregular arrangement can come from the imperfect epitaxial growth of the soot particles, due in turn to a variety of defects. Thus, soot particles show superimposed (defective) graphenic layers which can be curved, and can be seen only locally as approximately parallel. The structure shown by soot globules can be more loosely said to be "onion-like" to describe the arrangement of the graphenic layers.

[3] (a) Finlayson-Pitts, B. J.; Pitts, J. N. jr *Chemistry of the Upper and Lower Atmosphere*, Academic Press, **2000**, Chapter 10, sections E and F. (b) ibidem, Chapter 10, section A, § 4.

[4] (a) Homann, K.-H. *Angew. Chem. Int. Ed.* **1998**, *37*, 2434-2451. (b) Weilmünster, P.; Keller, A.; Homann, K.-H. *Comb. Flame* **1999**, 116, 62-83. (c) Keller, A.; Kovacs, R.; Homann, K.-H. *Phys. Chem. Chem. Phys*. **2000**, *2*, 1667-1675. (d) Fialkov, A. B.; Homann K.-H. *Comb. Flame* **2001**, 127, 2076-2090.

[5] Shi, Z.; Zhang, D.; Ji, H.; Hasegawa, S.; Hayashi, M. *Sci. Tot. Environ.* **2008**, *389*, 195-201.

[6] Lu're, B. A.; Mikhno A. V. *Kinetics & Catalysis* **1997**, *38*, 490-497.

[7] Pöschl, U.; Letzel, T.; Schauer, C.; Niessner, R. *J. Phys. Chem. A* **2001**, *105*, 4029-4041.

[8] Kamens, R. M.; Guo, J.; Guo, Z.; McDow, S. R. *Atmos. Environ*. **1990**, *24A*, 1161-1173.

[9] Kirchner, U.; Scheer, V.; Vogt, R. *J. Phys. Chem. A* **2000**, *104*, 8908-8915.

[10] Arens, F.; Gutzwiller, L.; Baltensperger, U.; Gäggeler, H. W.; Amman, M. *Environ. Sci. Technol.* **2001**, *35*, 2191-2199.

[11] Jung, J.; Lee, J. H.; Song, S.; Chun, K. M. *Int. J. Aut. Tech.* **2008**, *9*, 423-428.

[12] Popovicheva, O.; Persiantseva, N. M.; Shonija, N. K.; DeMott, P.; Koehler, K.; Petters, M. Kreidenweis, S.; Tishkova, V.; Demirdjian B.; Suzanne J. *Phys. Chem. Chem. Phys.* **2008**, *10*, 2332–2344.

[13] Fendel, W.; Matter, D.; Burtscher, H.; Schmidt-Ott, A. *Atmos. Environ.* **1995**, *29*, 967-973.

[14] Kamm, S.; Mohler, O.; Naumann K.-H.; Saathoff, H.; Schurath,U. *Atmos. Environ.* **1999**, *33*, 4651-4661.

[15] Stephens, S.; Rossi, J. M.; Golden, D.M. *Int. J. Chem. Kinet.* **1986**, *18*, 1133-1149. Fendel, W.; Matter, D.; Burtscher, H.; Schmidt-Ott, A. *Atmos. Environ.* **1995**, *29*, 967-973. Smith, D.M.; Chughtai, A. R. *J. Geophys. Res.*, **1996**, *101*, 19607-19620. Wei, C.-F.; Larson, S.; Patten, K.; Wuebbles, D. *Atmos. Environ.* **2001**, *35*, 6167–6180. Lelièvre, S.; Bedjanian, Y.; Pouvesle, N.;

Delfau, J.-L.; Vovelle, C.; Le Bras, G. *Phys. Chem. Chem. Phys.* **2004**, *6*, 1181-1191. Metts, T. A.; Battermann, S. A.; Fernandes, G. I.; Kalliokoski, P. *Atmos. Environ.* **2005**, *39*, 3343–3354.

[16] Disselkamp, R.S.; Carpenter, M. A.; Cowin, J.P.; Berkowitz, C.M.; Chapman, E.G.; Zaveri, R.A.; Laulainen, N.S. *J. Geophys. Res.*, **2000**, *105*, 9767-9771.

[17] Moriconi, E. G.; Rakocz, B.; O'Connor, W. F. *J. Am. Chem. Soc.* **1961**, *83*, 4618. Letzel T., Rosemberg, E.; Wissiack, R.; Grasserbauer, M.; Niessner, R. *J. Chrom.* A **1999**, *855*, 501-514. Kwamena, N.-O. A.; Thornton, J. A.; Abbatt, J. P. D. *J. Phys. Chem. A* **2004**, *108*, 11626-11634. Kwamena, N.-O. A.; Earp, M. E.; Young, C. J.; Abbatt, J. P. D. *J. Phys. Chem. A* **2006**, *110*, 3638-3646. Kwamena, N.-O. A.; Staikova, M. G.; Donaldson, D. J.; George, I. J.; Abbatt J .P. D. *J. Phys. Chem. A* **2007**, *111*, 11050-11058. McCabe, J.; Abbatt, J. P. D. *J. Phys. Chem. C* **2009**, *113*, 2120-2127. Kolasinski, K. W. *Surface Science*, John Wiley & Sons, LTD, **2002**, *Chapter 3*, section 3.14.1.

[18] (a) Perraudin, E.; Budzinski, H.; Villenave E. *Atmos. Environ.* **2007**, *41*, 6005-6017. (b) Perraudin, E.; Budzinski, H.; Villenave E. *J. Atmos. Chem.* **2007**, *56*, 57-82. (c) Miet, K.; Le Menach, K.; Flaud, P. M.; Budzinski, H.; Villenave, E. *Atmos. Environ*. **2009**, *43*, 3699-3707.

[19] Atkinson, R.; Arey, J. *Environ. Health Perspect.* **1994**, *102*, Suppl. 4, 117-126.

[20] Pitts, J. N. jr.; Lokensgard, D. M.;Ripley, P.S.; van Cauwenberghe, K. A.; van Vaeck, L.; Schaffer, S.D.; Thill, A. J.; Belser, W. L. *Science* **1980**, *210*, 1347-1349.

[21] Ghigo, G.; Tonachini, G. *J. Am. Chem. Soc.* **1998**, *120*, 6753-6757. Ghigo, G.; Tonachini, G. *J. Am. Chem. Soc.* **1999**, *121*, 8366-8372. Ghigo, G.; Tonachini, G. *J. Chem. Phys.* **1999**, *109*, 7298-7304. Motta, F.; G. Ghigo, G.; Tonachini, G. *J. Phys. Chem. A* **2002**, *106*, 4411-4422. Ghigo, G; Maranzana, A.; Causà, M.; Tonachini, G. *J. Phys. Chem. A* **2006**, *110*, 13270-13282.

[22] Montoya, A.; Truong, T. N.; Sarofim, A. F. *J. Phys. Chem. A* **2000**, 104, 6108-6110. Montoya, A.; Truong, T. N.; Sarofim, A. F *J. Phys. Chem. A* **2000**, 104, 8409-9417

[23] Frankcombe, J.; Smith, S. C. *Carbon* **2004**, *42*, 2921-2928.

[24] Chen, N.; Yang, R. T. *Carbon* **1998**, *36*, 1061-1070.

[25] Kiotani, T.; Tomita, A. *J. Phys. Chem. B* **1999**, *103*, 3434-3441.

[26] Sendt, K.; Haynes, B. S. *J. Phys. Chem. A* **2005**, *109*, 3438-3447.

[27] Radovic, L. R.; Bockrath, B. *J. Am. Chem. Soc.* **2005**, *127*, 5917-5927.

[28] Ghigo, G; Maranzana, A.; Tonachini, G.; Zicovich-Wilson, C. M.; Causà, M. *J. Phys. Chem. B* **2004**, *108*, 3215-3223.

[29] Maranzana, A.; Serra, G.; Giordana, A.; Tonachini, G.; Barco, G.; Causà, M. *J. Phys. Chem. A* **2005**, *109*, 10929-10939.

[30] Barco, G.; Maranzana, A.; Ghigo, G.; Causà, M.; Tonachini, G. *J. Chem. Phys.*, **2006**, *125*, 184706.

[31] Cash, G. G.; Dias, J.R. *J. Math.Chem.* **2001**, *30*, 429-444.

[32] Giordana, A.; Maranzana, A.; Ghigo, G.; Causà, M.; Tonachini, G. *J. Phys. Chem. A* **2008**, *112*, 973-982.

[33] Pople, J. A.; Gill, P. M. W.; Johnson, B. G. *Chem. Phys. Lett.* **1992**, *199*, 557-560. Schlegel, H. B. in *Computational Theoretical Organic Chemistry*, Csizsmadia, I. G.; Daudel, Eds., Reidel Publ. Co., **1981**, p.129-159; Schlegel, H. B. *J. Chem. Phys.* **1982**, *77*, 3676-3681; Schlegel, H. B.; Binkley, J. S.; Pople, J. A. *J. Chem. Phys.* **1984**, *80*, 1976-1981; Schlegel, H. B. *J. Comput. Chem*. **1982**, *3*, 214-218.

[34] Parr, R. G.; Yang, W. *Density Functional Theory of Atoms and Molecules*, Oxford University Press: New York, **1989**; Ch.3.

[35] Jensen, F. *Introduction to Computational Chemistry*, John Wiley & Sons, **1999**, Ch. 6.

[36] (a) Hehre, W. J.; Ditchfield, R.; Pople, J. A. *J. Chem. Phys.* **1972**, *56*, 2257-2261. Hariharan, P. C.; Pople, J. A. *Theor. Chim. Acta* **1973**, *28*, 213-222. (b) Gordon, M. S.; Binkley, J. S.; Pople, J. A.; Pietro W. J.; Hehre W. J. *J. Am. Chem. Soc.* **1982**, 104, 2797; Pietro, W. J.; Francl, M. M.; Hehre, W. J.; Defrees, D. J.; Pople, J. A.; Binkley, J. S. *J. Am. Chem. Soc.* **1982**, 104, 5039.

[37] Reed, A. E.; Weinstock, R. B.; Weinhold, F. *J. Chem. Phys.* **1985**, *83*, 735-746. Reed, A. E.; Weinhold, F. *J. Chem. Phys.* **1983**, *78*, 4066-4073. Foster, J. P.; Weinhold, F. *J. Am. Chem. Soc.* **1980**, *102*, 7211-7218.

[38] This procedure rather satisfactorily defines the singlet-triplet gap for dioxygen as 21.6 kcal mol^{-1}.

[39] Goldstein, E.; Beno, B.; Houk, K. N. *J. Am. Chem. Soc.* **1995**, *118*, 6036-6043. Yamanaka, S. ; Kawakami, T.; Nagao, K. ; Yamaguchi, K. *Chem. Phys. Lett.* **1994**, *231*, 25-33. Yamaguchi, K.; Jensen, F.; Dorigo, A.; Houk, K. N. *Chem. Phys. Lett.* **1988**, *149*, 537-542.

[40] Gaussian 03, Revision D.02. Frisch, M. J.; Trucks, G. W.; Schlegel, H. B.; Scuseria, G. E.; Robb, M. A.; Cheeseman, J. R.; Montgomery, Jr., J. A.; Vreven, T.; Kudin, K. N.; Burant, J. C.; Millam, J. M.; Iyengar, S. S.; Tomasi, J.; Barone, V.; Mennucci, B.; Cossi, M.; Scalmani, G.; Rega, N.; Petersson, G. A.; Nakatsuji, H.; Hada, M.; Ehara, M.; Toyota, K.; Fukuda, R.; Hasegawa, J.; Ishida, M.; Nakajima, T.; Honda, Y.; Kitao, O.; Nakai, H.; Klene, M.; Li, X.; Knox, J. E.; Hratchian, H. P.; Cross, J. B.; Bakken, V.; Adamo, C.; Jaramillo, J.; Gomperts, R.; Stratmann, R. E.; Yazyev, O.; Austin, A. J.; Cammi, R.; Pomelli, C.; Ochterski, J. W.; Ayala, P. Y.; Morokuma, K.; Voth, G. A.; Salvador, P.; Dannenberg, J. J.; Zakrzewski, V. G.; Dapprich, S.; Daniels, A. D.; Strain, M. C.; Farkas, O.; Malick, D. K.; Rabuck, A. D.; Raghavachari, K.; Foresman, J. B.; Ortiz, J. V.; Cui, Q.; Baboul, A. G.; Clifford, S.; Cioslowski, J.; Stefanov, B. B.; Liu, G.; Liashenko, A.; Piskorz, P.; Komaromi, I.; Martin, R. L.; Fox, D. J.; Keith, T.; Al-Laham, M. A.; Peng, C. Y.; Nanayakkara, A.;

Challacombe, M.; Gill, P. M. W.; Johnson, B.; Chen, W.; Wong, M. W.; Gonzalez, C.; and Pople, J. A.; Gaussian, Inc., Wallingford CT, **2004**.

[41] (a) Saunders, V.R.; Dovesi, R.; Roetti, C.; Orlando, R; Zicovich-Wilson, C.M.; Harrison, N.M.; Doll, K.; Civalleri, B.; Bush, I.J.; D'Arco, Ph; Llunell, M. *CRYSTAL 2003 User Manual,* **2003**, Turin University. (b) Saunders, V. R.; Dovesi, R.; Roetti, C.; Causà, M.; Harrison, N. M.; Zicovich-Wilson, C. M.; *CRYSTAL'98. User Manual*. **1999**, Turin University; (c) Pisani, C.; Dovesi, R.; Roetti, C. *Hartree-Fock ab-initio Treatment of Crystalline Systems, Lecture Notes in Chemistry vol. 48*, **1988**, Springer Verlag, Heidelberg.

[42] Dovesi, R.; Pisani, C.; Roetti, C.; Saunders, V. R. *Phys. Rev. B* **1983**, *28*, 5781-5792.

[43] Causà, M.; Dovesi, R.; Orlando, R.; Pisani, C.; Saunders, V. R. *J. Phys. Chem.* **1988**, *92*, 909-913.

[44] Pisani, C.; Aprà E.; Causà M. *Int. J. Quantum Chem.* **38**, 395-417 (1990).

[45] Zicovich-Wilson, C. M.; Dovesi, R. *Int. J. Quantum Chem* **1998,** *67*, 299-309.

[46] Doll, K.; Harrison, N. M.; Saunders, V. R. *Int. J. Quantum Chem.* **2001**, 82, 1-12; Doll, K. *Comput. Phys. Commun.* **2001**, *137*, 74-82; Civalleri, B.; D'Arco, Ph.; Orlando, R.; Saunders, V. R.; Dovesi, R. *Chem. Phys. Lett.* **2001**, *348*, 131-138.

[47] Blake, D. F.; Kato, K. *J. Geophys. Res.* **1995**, *100*, 7195-7202. Peuschl, R. F.; Boering, K. A.; Verma, S.; Howard, S. D.; Ferry, G. V.; Goodman, J.; Allen, D. A.; Hamill, P. *J. Geophys. Res.* **1997**, *102*, 13113-13118. Petzold, A.; Stein, C.; Nyeki, S.; Gysel, M.; Weingartner, E.; Baltensperger, U.; Giebl, H.; Hitzenberger, R.; Dopelheuer, A.; Vrchoticky, S.; Puxbaum, H.; Johnson, M:; Hurley, C. D.; Marsh, R.; Wilson, C. W. *Geophys. Res. Lett.* **2002,** *30*, 1719-1722. Grothe, H.; Muckenhuber, H. *The Third Informal Conference on Reaction Kinetics and Atmospheric Chemistry*, **2002** Helsingør, Denmark. Kamm, S.; Saathoff, H.; Naumann, K. H.; Mohler, O.; Schurath, U. *Comb. Flame* **2004**, *138*, 353-361, and references therein. Harris, P. J. F. *Crit. Rev. Solid State and Mat. Sci.* **2005**, *30*, 235-253. Sadezky, A.; Muckenhuber H.; Grothe, H.; Niessner, R.; Pöschl, U. *Carbon* **2005** *43*, 1731-1742. Muckenhuber, H.; Grothe, H. *Carbon* **2007**, *45*, 321-329. Liu, L.; Rim, K. T.; Eom, D.; Heinz, T. F.; Flynn, G. W. *Nano Lett.* **2008**, *8*, 1872-1878. Jäger, C.; Huisken, F.; Mutschke, H.; Llamas Jansa, I.; Henning, Th. *Astrophys. J.* **2009**, 696, 706–712.

[48] Saathoff, H.; Moehler, O.; Schurath, U.; Kamm, S.; Dippel, B.; Mihelic, D. *J. Aerosol Sci.* **2003**, *34*, 1277-1296.

[49] Dias, J. R. *J. Chem. Inf. Model.* **2005**, *45*, 562-571.

[50] Salem, L. *Electrons in Chemical Reactions*, Ch. 7, § 4, John Wiley & Sons, **1982**.

[51] The 1,4 PO, located 27 kcal mol^{-1} above R, presents a 7-membered ring, resulting from addition to the **cc** positions. The related concerted attack, representative of a [π4 + π4] *forbidden*

cycloaddition, comes out to correspond to a second order saddle point. Finally, since the 1,3 attack (involving one **c** and the distal **a** position) produces a 6-ring PO located at 37 kcal mol^{-1} above R, no TS search was carried out for this position, since it would imply a barrier higher than 18 kcal mol^{-1}.

52 O_2 loss could occur with different outcomes, depending on the spin multiplicity. ^{1}POD could lose ground state dioxygen only with formation of a triplet oxyl diradical, ^{3}OD, in an almost isoergic step (-0.3 kcal mol^{-1}). But the relevant barrier for TS ^{1}POD-^{3}OD is 13.7 kcal mol^{-1} high with respect to ^{1}POD. If an ISC could occur, $^3O_2$ loss from ^{3}POD (lower in energy than ^{1}POD by 0.9 kcal mol^{-1}) would produce ^{1}EPO. But the barrier for TS ^{3}POD-^{1}EPO is 14.8 kcal mol^{-1} high with respect to ^{3}POD, though the dissociation limit $^3O_2$ + ^{1}EPO is 15.5 kcal mol^{-1} below ^{3}POD.

53 Smith, D. M.; Chughtai, A. R. *J. Atmos. Chem.* **1997**, *27*, 77-91. Chughtai, A. R.; Welch, W. F.; Akhter, M. S.; Smith, D. M. *Appl. Spectr.* **1990**, *44*, 175-336. Sergides, C. A.; Jassim, J. A.; Chughtai, A. R.; Smith D. M. *Appl. Spectrosc.* **1987**, *41*, 482-492.

54 An alternative could be producing ^{1}EPO via $^1O_2$ loss. However, such a TS could not be found, since any attempt produced TS ^{1}TD-^{3}OD. The ^{1}EPO plus $^1O_2$ limit is located at -17.9 kcal mol^{-1}.

55 The ^{3}EPO + $^3O_2$ limit is located at -8.0 kcal mol^{-1} below ^{1}TD, i.e. somewhat less stable than the ^{3}OD + $^3O_2$ dissociation limit. Then, considering the further evolution of ^{3}OD, negligible *G* barriers are found in correspondence of two (1,2) migrations of the hydrogen geminal to the O atom (Figure 3b). The first H shift is to the oxygen atom: here the *G* barrier estimate comes out to be negative by a small amount, -0.3 kcal mol^{-1} with respect to $^3O_2$ + ^{3}OD. It produces a phenol (^{3}PH, -29.8 kcal mol^{-1} below ^{1}TD). The second H shift is to the neighbouring carbon atom (barrier 0.5 kcal mol^{-1} with respect to $^3O_2$ + ^{3}OD), and gives a ketone, ^{3}KE, ca. 39.5 kcal mol^{-1} below ^{1}TD. In this case, the step to the keton is as easy as that to PH.

56 Actually, in the **M13** model, the trioxyl adduct from the attack onto the "allylic" central position is, not unexpectedly, found at 32.5 kcal mol^{-1} above that in the terminal position (it presents a triradical situation). For **M19**, data are reported for the trioxyl radical in the **c** position.

57 On the central position, the peroxyl radical is not stable and dissociates spontaneously; if a constrained optimization is carried out, with the C–O bond length frozen at 1.61 Å, a structure positioned at 50 kcal mol^{-1} above the reactants is found.

58 Barone, V.; Hod, O.; Scuseria, G. E. *Nano Lett.* **2006**, *6*, 2748-2754. Han., M.Y.; Özyilmaz, B.; Zhang, Y.; Kim, P. *Phys. Rev. Lett.* **2007**, *98*, 206805.

FIGURES 1-4 (free energy profiles)

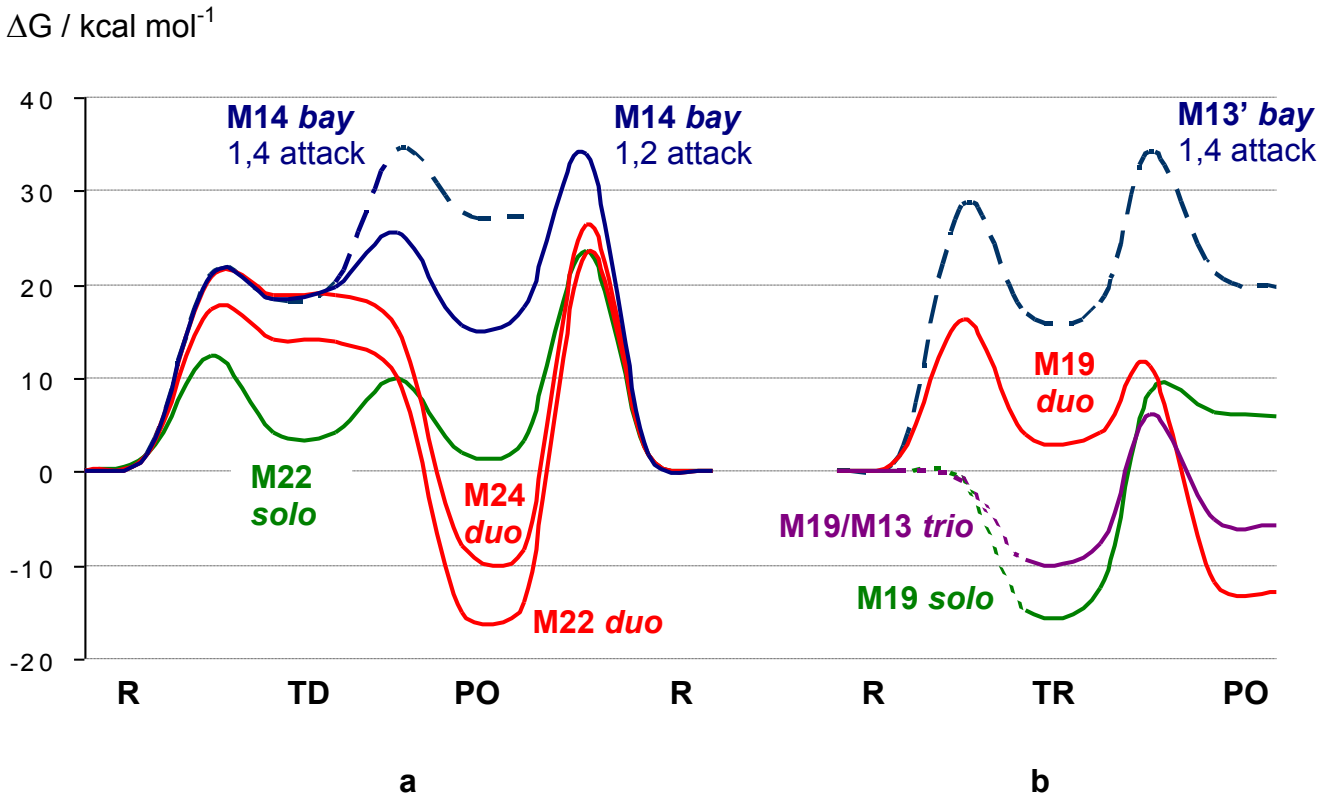

FIGURE 1. Free energy profiles for the initial O_3 attacks on (a) closed shell and (b) open shell PAH systems. The lines for **M13** and **M19** *trio* result superimposed. *Trio* and *solo* curves: dashes indicate portions of the *E* surface where an all-downhill steep reaction pathway is found (*G* not determined).

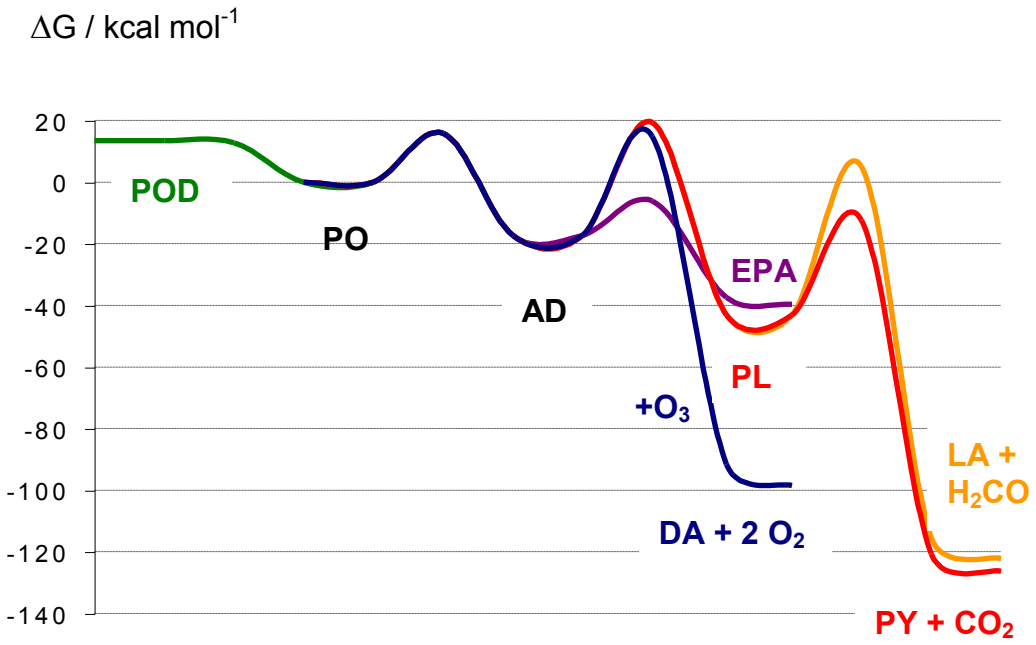

FIGURE 2. Free energy profiles for PO evolution in **M24** (*duo* position)..

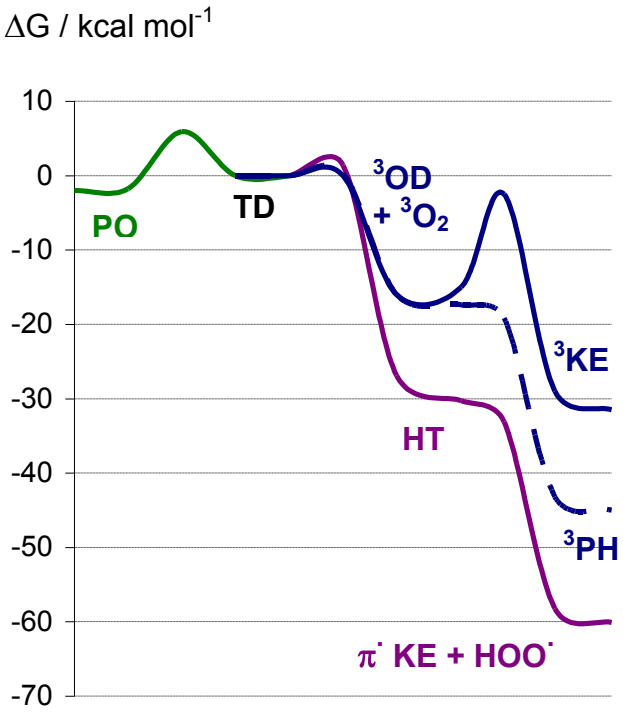

a

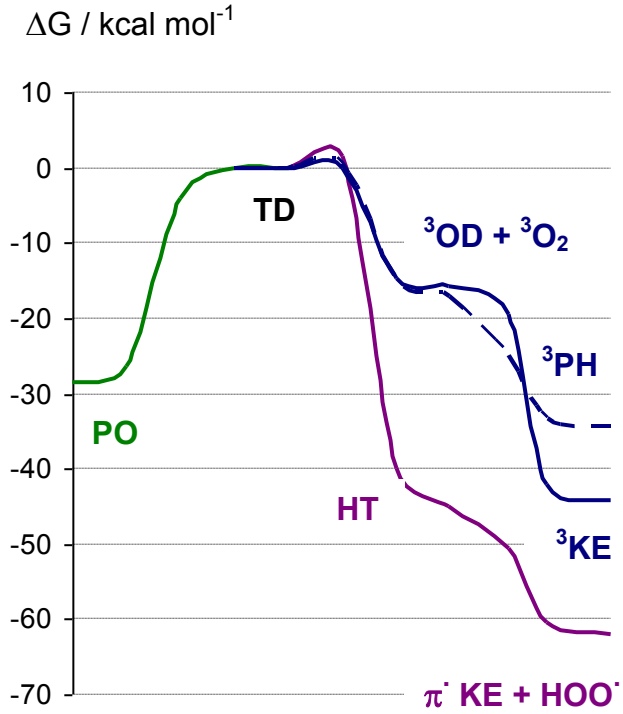

b

FIGURE 3. Free energy profiles for the further evolutions of TD in even PAH systems: (a) **M22** (*solo* position) and (b) **M24** (*duo* position).

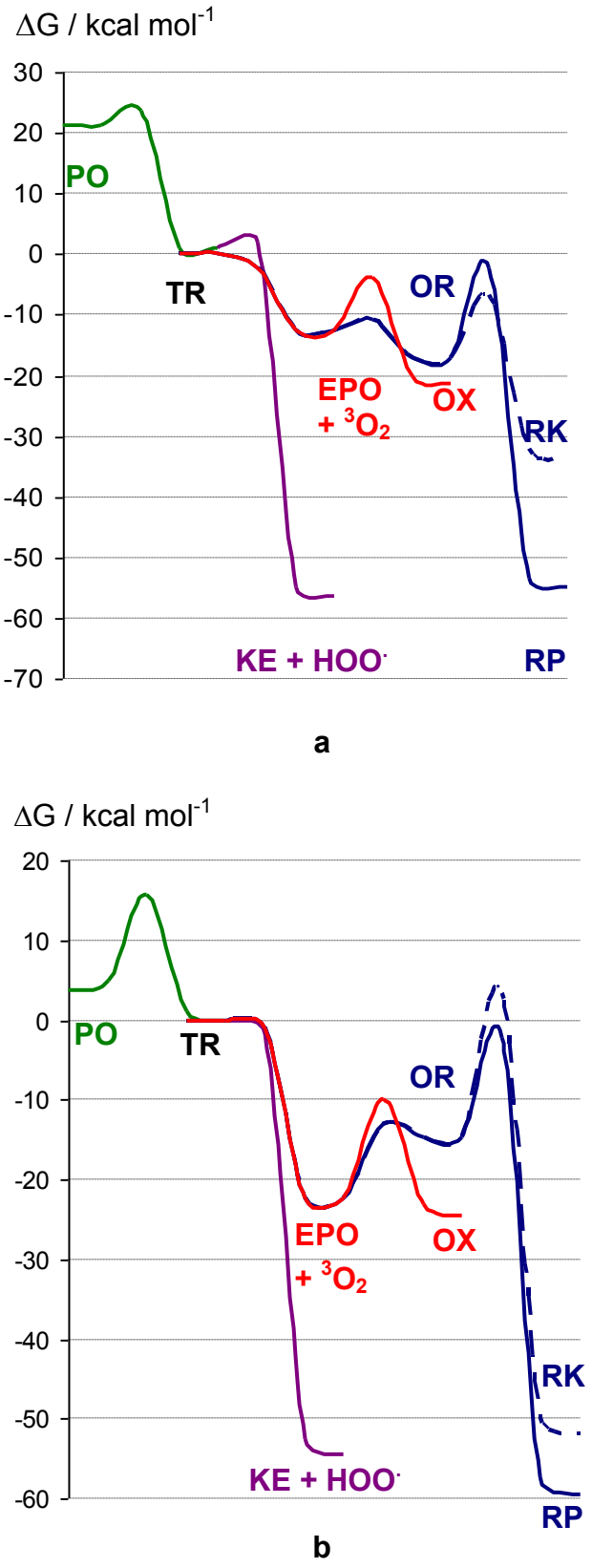

FIGURE 4. Free energy profiles for the further evolutions of TR in the open shell PAH system **M19** (*solo*, **a**, and *trio*, **b**, positions).

SCHEMES 1-3

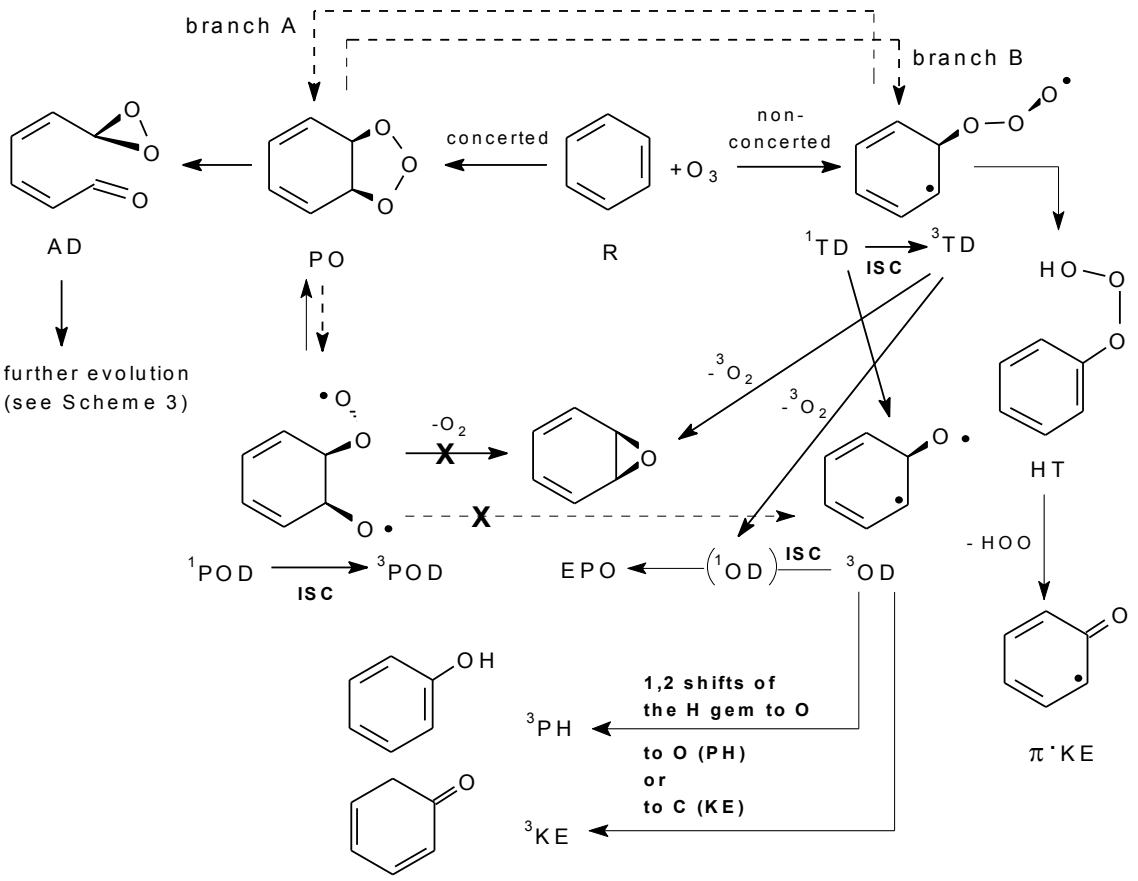

Scheme 1. **Even systems**. Conceivable pathways explored for the molecules in Chart 1 (symbolically represented by a single 6-membered ring).

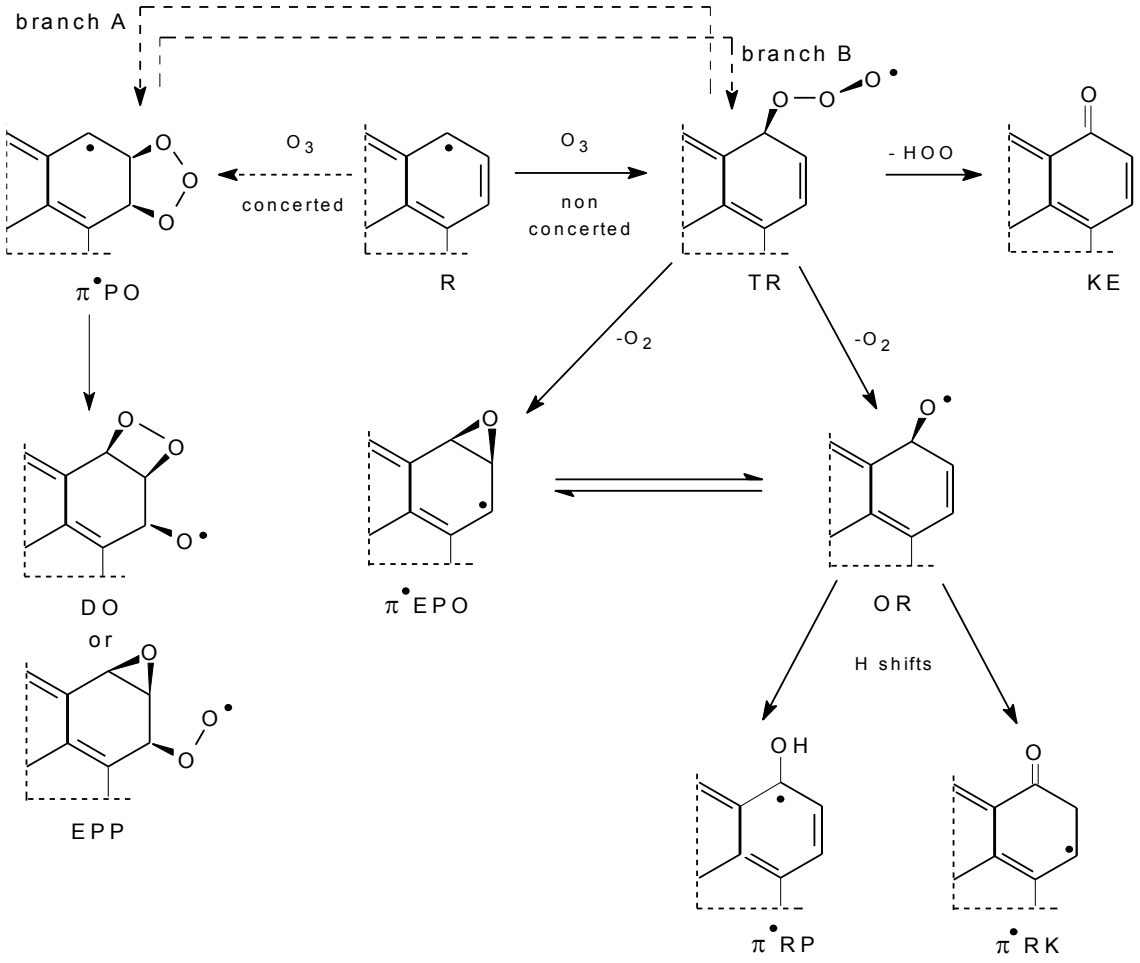

Scheme 2. Odd systems. Conceivable pathways explored for the molecules in Chart 1 (the scheme focuses on a single 6-membered ring).

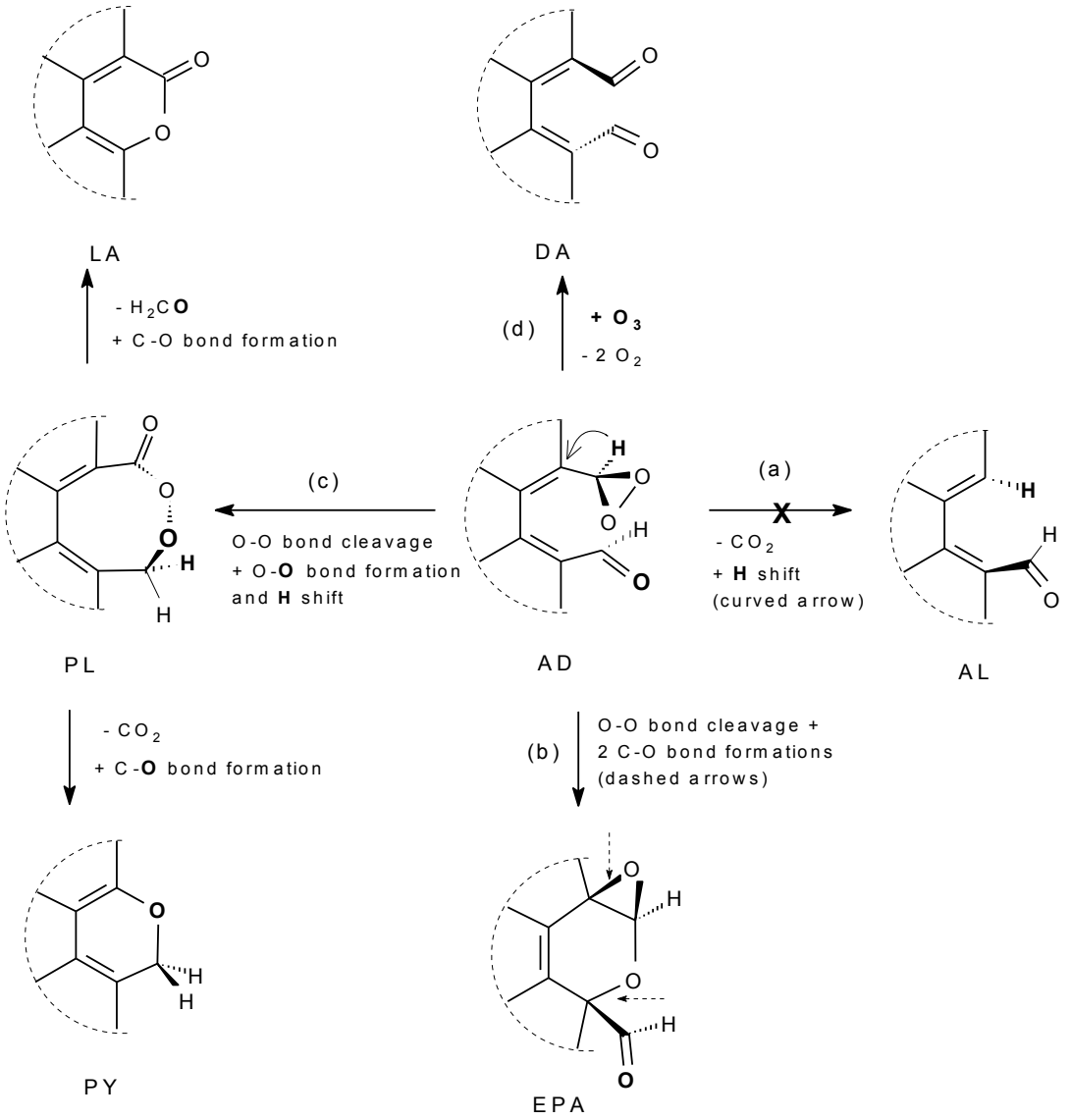

Scheme 3. Further steps from AD in **M24** (which is shown only partially, dashed contour).

CHARTS 1-3

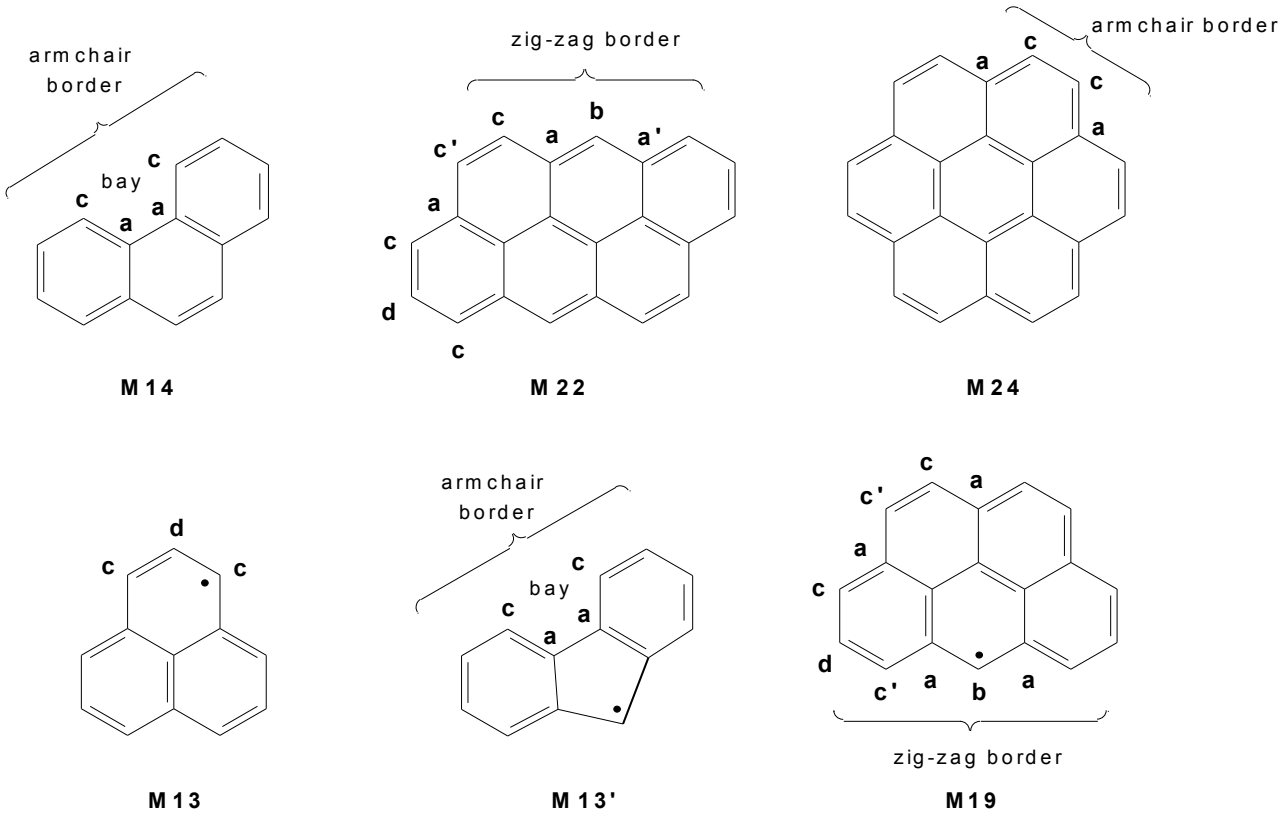

Chart 1: **Even molecular models** (top): phenanthrene (**M14**), anthanthrene (**M22**), and coronene (**M24**). **Odd molecular models** (bottom): the phenalenyl radical, **M13**, the fluorenyl radical (**M13'**), and the benzo[*cd*]pyrenyl radical, **M19**. All are shown by a single resonance structure. Letters label peripheral positions following this convention: **a** = tertiary carbons, **b** = secondary carbons between two tertiary carbons; **c** = secondary carbons between a tertiary carbon and a secondary carbon; **d** = secondary carbons between two secondary carbons.

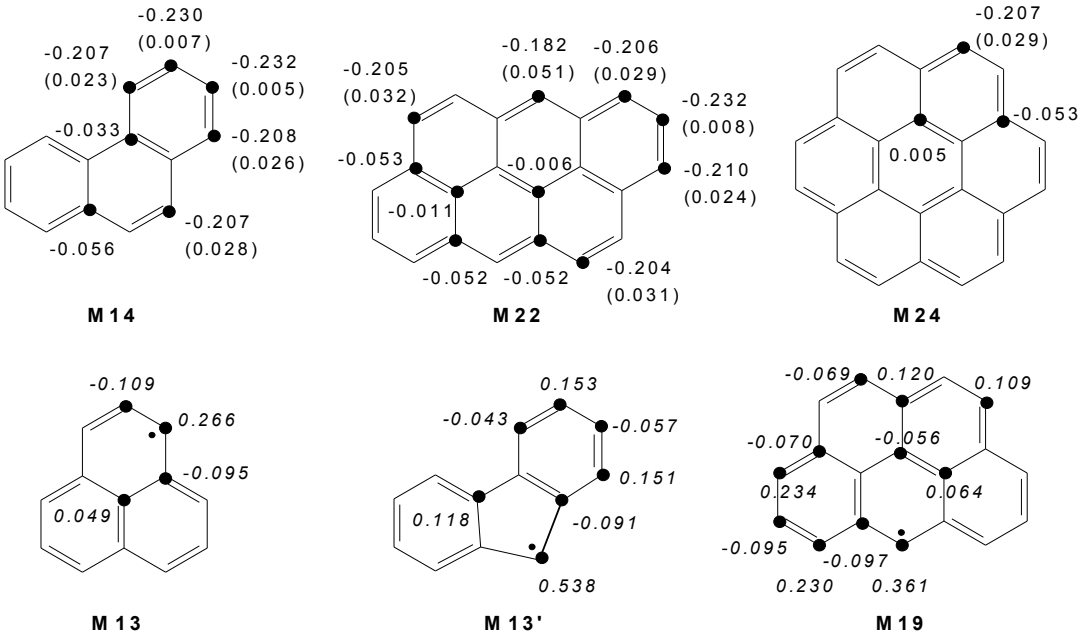

Chart 2: **Even models** (upper line): NAO charges on border carbons (CH group charges in parentheses) for phenanthrene (**M22**), anthanthrene (**M22**) and coronene (**M24**). **Odd models** (lower line): NAO spin densities (italic) on border carbons for the phenalenyl radical (**M13**), the fluorenyl radical (**M13'**), and the benzo[*cd*]pyrenyl radical (**M19**).

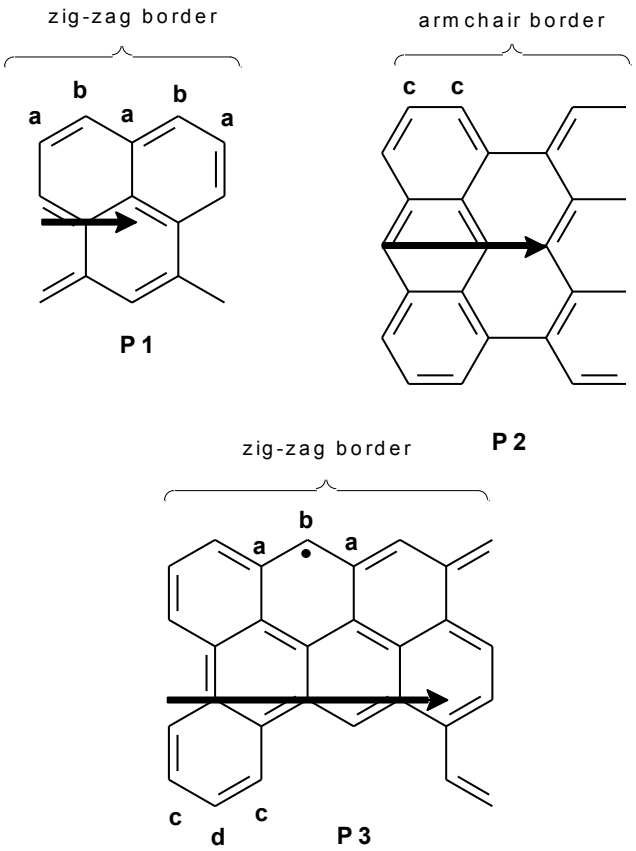

Chart 3: Periodic models. Arrows indicate the adopted elementary cells. Letters label peripheral positions mentioned in the text.